Antiferromagnetic planar-rotator model with further-neighbor interactions

Robert G. Caflisch*
Department of Physics, University of Rhode Island, Kingston, Rhode Island 02881
(Received 24 December 1987; revised manuscript received 10 July 1989)

An analysis has been made of the planar-rotator model in the presence of a magnetic field and further-neighbor interactions. A variety of new phases have been observed and described. A partial classification of the global phase diagram has been made as well as experimental realizations.

I. INTRODUCTION

In this paper I will use mean-field theory (see Refs. 1 and 2, and references therein) to address the problem of competing interactions at different length scales in planar-rotator systems, and explicitly focus on the triangular lattice with three nearest neighbors (see Fig. 1) and a magnetic field. This work is motivated by experimental work[3] in which $2\sqrt{3}\times 2\sqrt{3}$ ordering was observed in $MnCl_2$ intercalated graphite. Such an ordering clearly requires scales larger than the $\sqrt{3}\times\sqrt{3}$ displacement of the nearest-neighbor problem.

Whereas the critical properties are not obtained precisely, this method does have the benefit of yielding considerable information about the structures formed while allowing an analytic analysis of the thermodynamics. Ground-state analyses have been performed for the second-neighbor triangular lattice model by Katsura, Ide, and Morita.[4]

II. THEORY

A. General case

I will perform an analysis of the (reduced) Hamiltonian

$$H \equiv \sum_{\langle k,j\rangle} J_{kj}\cos(\theta_k-\theta_j)-\sum_k h_k\cos(\theta_k-\sigma_k)\ , \tag{1}$$

where $\langle k,j\rangle$ runs over the neighboring (i.e., interacting) pairs of sites of a not yet specified lattice, and θ_k is the angle for a spin on the kth site. The direction of the magnetic field on the kth site is the angle σ_k. The temperature (T) has been absorbed into the coefficients of H by choosing $H\equiv E/(k_BT)$, where E is the energy. The method is similar to that described in earlier more restricted models.[1,2] I will attempt to minimize the functional

$$\Psi[\rho]\equiv \mathrm{Tr}_{\theta}\{\rho(\boldsymbol{\theta})H(\boldsymbol{\theta})+\rho(\boldsymbol{\theta})\ln[\rho(\boldsymbol{\theta})]\} \tag{2}$$

with respect to a normalized probability distribution $\rho(\boldsymbol{\theta})$. Here, $\boldsymbol{\theta}$ is the vector containing the spins of all the sites, and Tr_{θ} is the trace over all values of $\boldsymbol{\theta}$. The variational analysis is done within the restricted set of probabilities

$$\rho(\boldsymbol{\theta})\equiv\prod_k \rho_k(\theta_k)\ . \tag{3}$$

All the solutions of the variational equations have the form

$$\rho_k(\theta_k)=e^{a_k\cos(\theta_k-\phi_k)}/[2\pi I_0(a_k)] \tag{4}$$

with $a_k\geq 0$ and $0\leq\phi_k\leq 2\pi$, and I_n is the nth modified Bessel function of the first kind. This form is independent of both the lattice and the J_{kj}'s. The average magnetization of the kth site can be most easily described in the complex formulation, with

$$M_k\equiv M_{k,x}+iM_{k,y}=\mathrm{Tr}_{\theta_k}e^{i\theta_k}\rho_k(\theta_k)=R(a_k)e^{i\phi_k}\ , \tag{5}$$

where $R(x)\equiv I_1(x)/I_0(x)$ (see Fig. 2), and $M_{k,x},M_{k,y}$ are the (real) x,y components of the magnetization of the kth site. Knowing M_k is exactly equivalent to knowing both a_k and ϕ_k. The magnetization per site is defined as $M\equiv\sum_k M_k/N$, where N is the number of sites. The self-consistent equations (SCE's) that relate the a_k's and ϕ_k's are found to be

$$a_k e^{i\phi_k}=h_k e^{i\sigma_k}-\sum_j J_{kj}M_j\ . \tag{6}$$

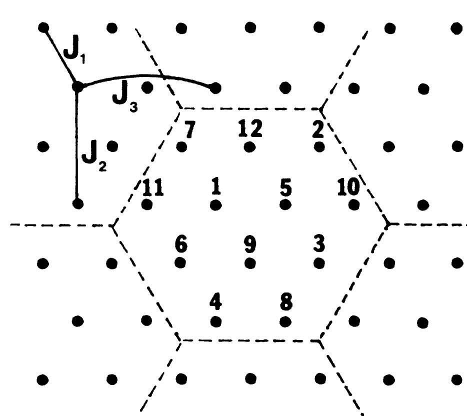

FIG. 1. The unit cell considered for the triangular lattice is shown. The sites are indexed so that {1,2,3,4}, {5,6,7,8}, and {9,10,11,12} are the $\sqrt{3}\times\sqrt{3}$ sublattices; and {1,8,10}, {2,7,9}, {3,6,12}, and {4,5,11} are the 2×2 sublattices. The displacements for the pair interactions J_1, J_2, and J_3 are shown.

The free energy [Eq. (2)] then becomes

$$\Psi[\rho]=\mathrm{Re}\left[\sum_{\langle kj\rangle} J_{kj}R(a_k)R(a_j)e^{i(\phi_k-\phi_j)} - \sum_k h_k e^{i(\phi_k-\sigma_k)}R(a_k) + \sum_k \{a_kR(a_k)-\ln[2\pi I_0(a_k)]\}\right], \quad (7)$$

where Re represents the real part of the argument. Inserting the SCE's one finds

$$\Psi=\sum_k \{\tfrac{1}{2}a_kR(a_k)-\tfrac{1}{2}\mathrm{Re}(h_ke^{-i\sigma_k}M_k)-\ln[2\pi I_0(a_k)]\}\ . \quad (8)$$

This last form is only correct as long as the values of a_k and ϕ_k satisfy the SCE's, and must *not* be treated as a quantity to variationally minimize. However, this form uncouples the sites and is useful in comparing multiple roots of the SCE's.

It can be seen from Eq. (7) that by *globally* rotating the spins by $\Delta\phi$ [i.e., $\tilde{\rho}(\theta)\equiv\rho(\theta-\Delta\phi)$, where $\Delta\phi_k=\Delta\phi$ for all k], the free energy may be written

$$\Psi[\tilde{\rho}]=-\mathrm{Re}\left[e^{i\Delta\phi}\sum_k h_ke^{-i\sigma_k}M_k[\rho]\right]+\cdots\ , \quad (9)$$

where the ellipsis represent terms invariant under $\Delta\phi$. Here $M_k[\rho]$ indicates the value of M_k in the distribution ρ. If $\sum_k h_ke^{-i\sigma_k}M_k$ does not lie on the non-negative real

TABLE I. Summary of the properties of the allowed solutions of the self-consistent equations. The individual phases are preceded by a number in parentheses, and are grouped together under common classes. For some of the phases the free energy cannot be expressed simpler than Eqs. (7) and (8) and has not been listed here. Here $\Phi(\kappa)\equiv\frac{1}{2}\alpha(\kappa)^2/\kappa-\ln[2\pi I_0(\alpha(\kappa))]$.

Phase	Degeneracy	Symmetry and conditions	Free energy per site
(1) Paramagnetic	1	$a_k=a,\phi_k=0$, for all k $a=h-(6J_1+6J_2+6J_3)R(a)$	$-(3J_1+3J_2+3J_3)R^2(a)$ $-\ln[2\pi I_0(a)]$
2×2:		$M_1=M_8=M_{10},M_2=M_7=M_9$, $M_3=M_6=M_{12},M_4=M_5=M_{11}$	
(2) Continuum	∞	$a_k=\alpha(2J_1+2J_2-6J_3)$, for all k $h=(8J_1+8J_2)R(a_1)\sum_{k=1}^{4}e^{i\phi_k}/4$	$\Phi(2J_1+2J_2-6J_3)$ $-h^2/(16J_1+16J_2)$
(Ferrimagnetic)		$\tilde{a}_k-(2J_1+2J_2-6J_3)R(\tilde{a}_k)=h-(8J_1+8J_2)M$, $\tilde{a}_k\equiv a_ke^{i\phi_k}$ ($\tilde{a}_k$ is real), $\phi_k=0$ *or* π, $k=1,2,3,4$	
(3) $c2\times2$	4	$a_2=a_3=a_5\neq a_1$	
(4) biaxial 2×2	12	$a_1\neq a_2\neq a_3=a_5$	
(5) 2×1	6	$a_1=a_2\neq a_3=a_5$	
$\sqrt{3}\times\sqrt{3}$:		$M_1=M_2=M_3=M_4$, $M_8=M_7=M_6=M_5$, $M_{10}=M_9=M_{12}=M_{11}$,	
(Continuum)		$a_k=\alpha(3J_1-6J_2+3J_3)$, for all k $h=(9J_1+9J_3)R(a_1)\sum_{k=1,5,9}e^{i\phi_k}/3$	$\Phi(3J_1-6J_2+3J_3)$ $-h^2/(18J_1+18J_3)$
(6) Nonhelical	∞	$\sum_{k=1,5,9}e^{i\phi_k}<1$	
(7) Helical	$\infty\times2$	$\sum_{k=1,5,9}e^{i\phi_k}>1$	
(Ferrimagnetic)		$\tilde{a}_k-(3J_1-6J_2+3J_3)R(\tilde{a}_k)=h-(9J_1+9J_3)M$, $\tilde{a}_k\equiv a_ke^{i\phi_k}$($\tilde{a}_k$ is real), $\phi_k=0$ *or* π, $k=1,5,9$	
(8) Helical	6	$a_1\neq a_2\neq a_3\neq a_1$	
(9) Nonhelical	3	$a_1\neq a_2=a_3$	
(10) $2\sqrt{3}\times\sqrt{3}$	?	$M_1=M_2,M_3=M_4,M_5=M_6$, $M_7=M_8,M_9=M_{10},M_{11}=M_{12}$,	
$2\sqrt{3}\times2\sqrt{3}$:			
(11) Uniform [Continuum(?)]	?	$a_k=\alpha(-J_1+2J_2+3J_3)$, for all k $h=(5J_1+8J_2+9J_3)R(a_1)\sum_{k=1}^{12}e^{i\phi_k}/3$	$\Phi(-J_1+2J_2+3J_3)$ $-h^2/(10J_1+16J_2+18J_3)$
(12) Nonuniform	?		

axis, then there is a value of $\Delta\phi$ such that $\Psi[\tilde{\rho}]$ is even less. This is true for any set of h_k's and J_{kj}'s. Thus, $\sum_k h_k e^{-i\sigma_k} M_k$ must be real and non-negative.

It should be said here that the above formalism is valid for both antiferromagnetic and ferromagnetic bonds. However, the interesting structural ordering is only expected for the cases with at least one non-negligible antiferromagnetic interaction.

It is usually necessary to further restrict the possible ρ's by assuming some sort of periodicity for ρ_i. However, this is caused by the computational difficulty of solving for so many variables, and not by any incompleteness of the SCE's.

B. Triangular lattice

Now, I consider the case where J_{kj} allows for first (J_1), second (J_2), and third (J_3) neighbor interactions (see Fig. 1), and the magnetic field is uniform ($h_k = h$, $\sigma_k = 0$ for all k). Without loss of generality take $h > 0$. The observed $2\sqrt{3}\times 2\sqrt{3}$ phase gives a unit cell as suggested in Fig. 1. I will thus restrict myself to this periodicity for the remainder of this paper. Such a restriction allows six possible periodicities: 1×1 (paramagnetic), 2×2, 2×1, $\sqrt{3}\times\sqrt{3}$, $2\sqrt{3}\times\sqrt{3}$, and $2\sqrt{3}\times 2\sqrt{3}$. The 2×1 case, however, is actually a special case of the 2×2 phase and the analysis shows it to be completely degenerate with the 2×2 phase. Thus, the 2×1 phase will not be treated independently. The results are summarized in Table I.

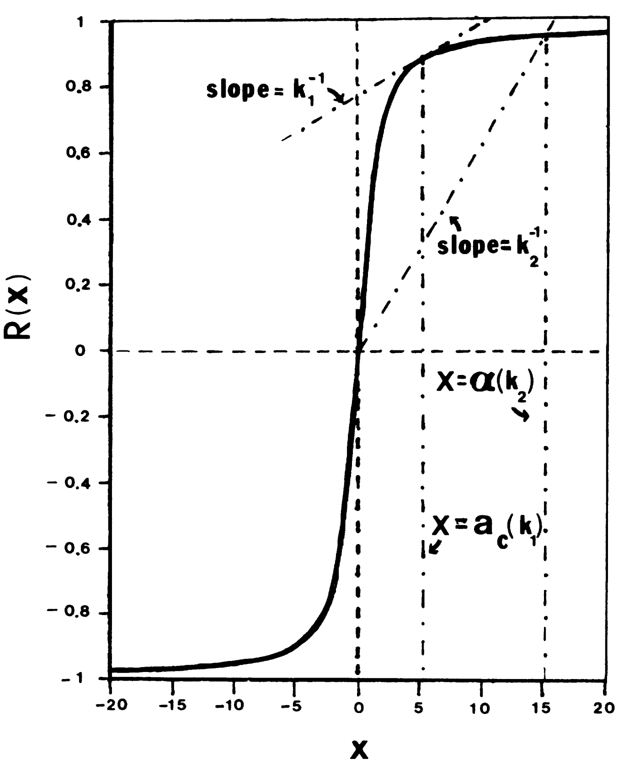

FIG. 2. The functions $R(x) \equiv I_1(x)/I_0(x)$ is shown. The related functions $\alpha(\kappa)$ and $a_c(\kappa)$ are illustrated. The line of slope κ_1^{-1} is $C(\kappa_1) = x - \kappa_1 R(a_c(\kappa_1))$.

Some of the fundamental equations are of the form $x - \kappa R(x) = c$, which has either one or three solutions, depending on κ and $|c|$ (see Fig. 2). To have three roots $[x_i(\kappa,c),\ i=1,2,3]$ requires $\kappa > 2$ and $|c| < C(\kappa)$, where $C(\kappa) = a_c(\kappa) - \kappa R(a_c(\kappa))$ and $a_c(>0)$ is defined by $R'(a_c(\kappa)) = \kappa^{-1}$. These roots then obey $x_1 \le -a_c \le x_2 \le a_c \le x_3$. Also, $x_2(\kappa,c) > 0$ if and only if $c > 0$.

Another fundamental equation, $x = \kappa R(x)$ always has the solution $x = 0$. For $\kappa > 2$, there is exactly one positive root $\alpha(\kappa)$. Some states are of this form: $a_k = \kappa R(a_k)$. Because the sites have been decoupled in Eq. (8), clearly (for these states) all sites prefer $a_k = 0$ or all sites prefer $a_k = \alpha(\kappa)$. The solution consisting of all zeros is paramagnetic (1×1) and is considered elsewhere.

1. *Uniform continuum states*

Assume that $a_j = a$ for all j, and $\kappa = a/R(a)$. Then the SCE's can be written in a matrix equation

$$\sum_l (\kappa\delta_{jl} + J_{jl}) e^{i\phi_l} R(a) = h \quad \text{for all } j\ . \tag{10}$$

If the matrix $\kappa\delta_{kl} + J_{kl}$ is nonsingular, then all the $e^{i\phi_l}$'s are real and uniquely determined. Of course, the constraint $|e^{i\phi_l}| = 1$ must be enforced for any "solution" of this matrix equation. Thus there may be cases with no solutions. The interesting solutions are associated with κ such that the matrix is singular. A tedious, but straightforward calculation gives those values (see Table II). I have accounted for all of these continua as associated with corresponding continuum phases.

2. *$2\sqrt{3}\times 2\sqrt{3}$ phases*

Due to the complexity of solving for 24 variables from 24 equations, it is not possible to say much about *all* $2\sqrt{3}\times 2\sqrt{3}$ solutions. But it is possible to look at specific types of solutions. Because of the existence of continuum states for the 2×2 and $\sqrt{3}\times\sqrt{3}$ phases, a logical guess is to try the form $a_k = a$ for all k. Under these conditions the SCE's may be written

TABLE II. The uniform continuum solutions are given, where $\kappa = a/R(a)$. κ is the eigenvalue of the matrix $-J_{kl}$, and its degeneracy is related to the dimension of the corresponding continuum.

κ	Degeneracy	Phase
$-6J_1 - 6J_2 - 6J_3$	1	Paramagnetic
$2J_1 + 2J_2 - 6J_3$	3	2×2 continuum
$3J_1 - 6J_2 + 3J_3$	2	$\sqrt{3}\times\sqrt{3}$ continuum
$-J_1 + 2J_2 + 3J_3$	6	$2\sqrt{3}\times 2\sqrt{3}$ continuum

$$e^{i\phi_k}[a-R(a)(-J_1+2J_2+3J_3)]=h-R(a)\{J_1[S_1-S_2(k)-S_{\sqrt{3}}(k)]+J_2 2S_{\sqrt{3}}(k)+J_3 3S_2(k)\} \tag{11}$$

for all k, where $S_1 \equiv \sum_{l=1}^{12} e^{i\phi_l}$. Here $S_2(k)$ and $S_{\sqrt{3}}(k)$, respectively, are defined as the sums of $e^{i\phi_l}$ over sites l (in the unit cell) on the 2×2 and $\sqrt{3}\times\sqrt{3}$ sublattices, respectively, containing k. In analogy with other solutions, if the left-hand side of Eq. (11) is zero, then except for special values of the J_n's, it follows that $4S_2(k)=3S_{\sqrt{3}}(k)=S_1=12M/R(a)$, for all k, and $h=(5J_1+8J_2+9J_3)M$. Solutions do exist for all h such

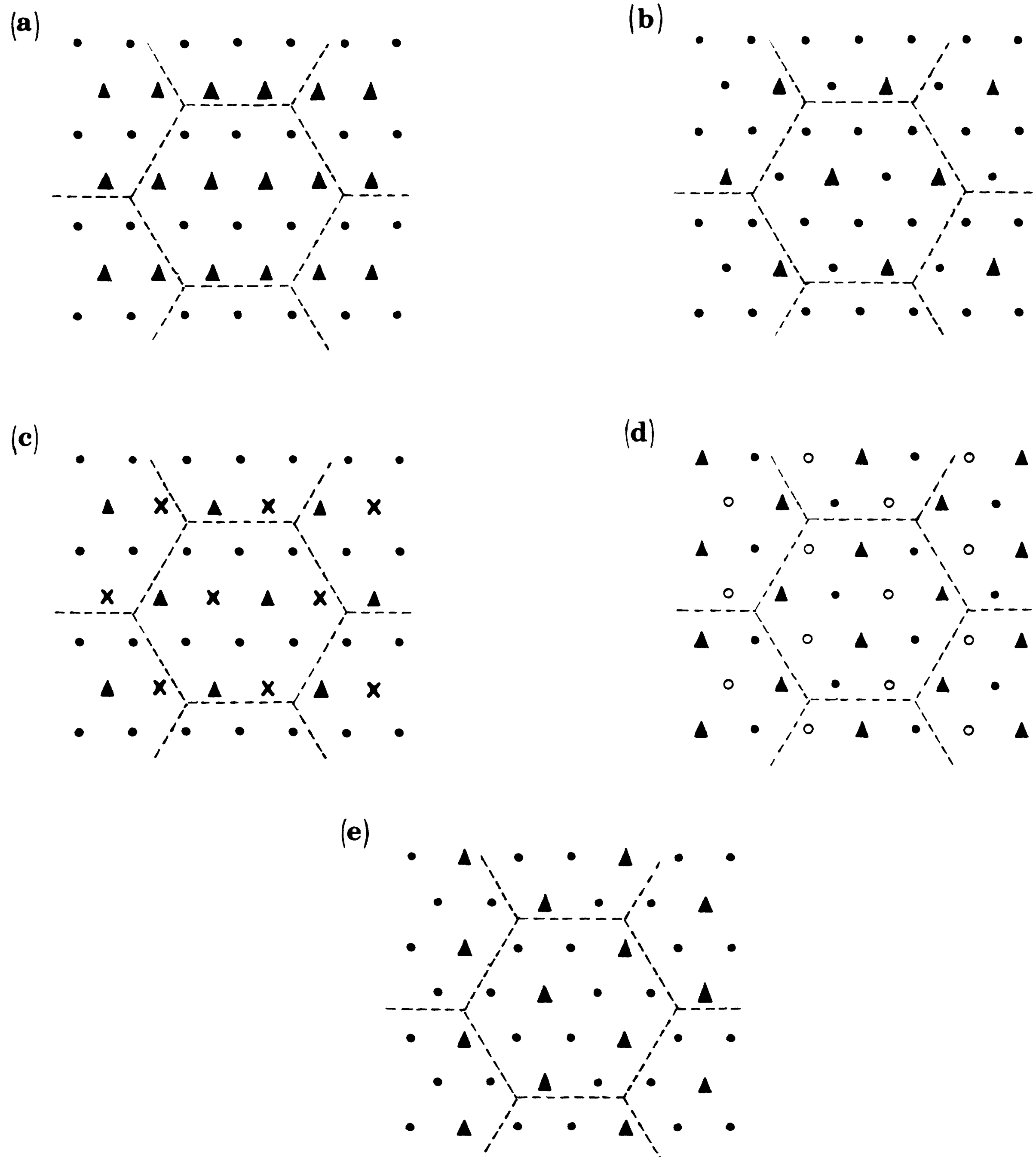

FIG. 3. The symmetries of the ferrimagnetic solutions are shown. Here, different symbols must have different values of the site magnetization. The phases are (a) 2×1; (b) $c2\times 2$; (c) biaxial 2×2; (d) helical $\sqrt{3}\times\sqrt{3}$; and (e) nonhelical $\sqrt{3}\times\sqrt{3}$.

that $|M/R(a)| < 1$.

At $h=0$, all the solutions [except those described later in Eq. (12)] have the form $\phi_k = \eta_k + \mu_k$, where η_k has 2×2 symmetry and μ_k has $\sqrt{3}\times\sqrt{3}$ symmetry, and $S_2(k) = S_{\sqrt{3}}(k) = 0$ is required. I call these solutions factorized continua. This is valid only for $h=0$, but clearly a small nonzero h cannot instantly make higher-symmetry phases thermodynamically preferable, if this

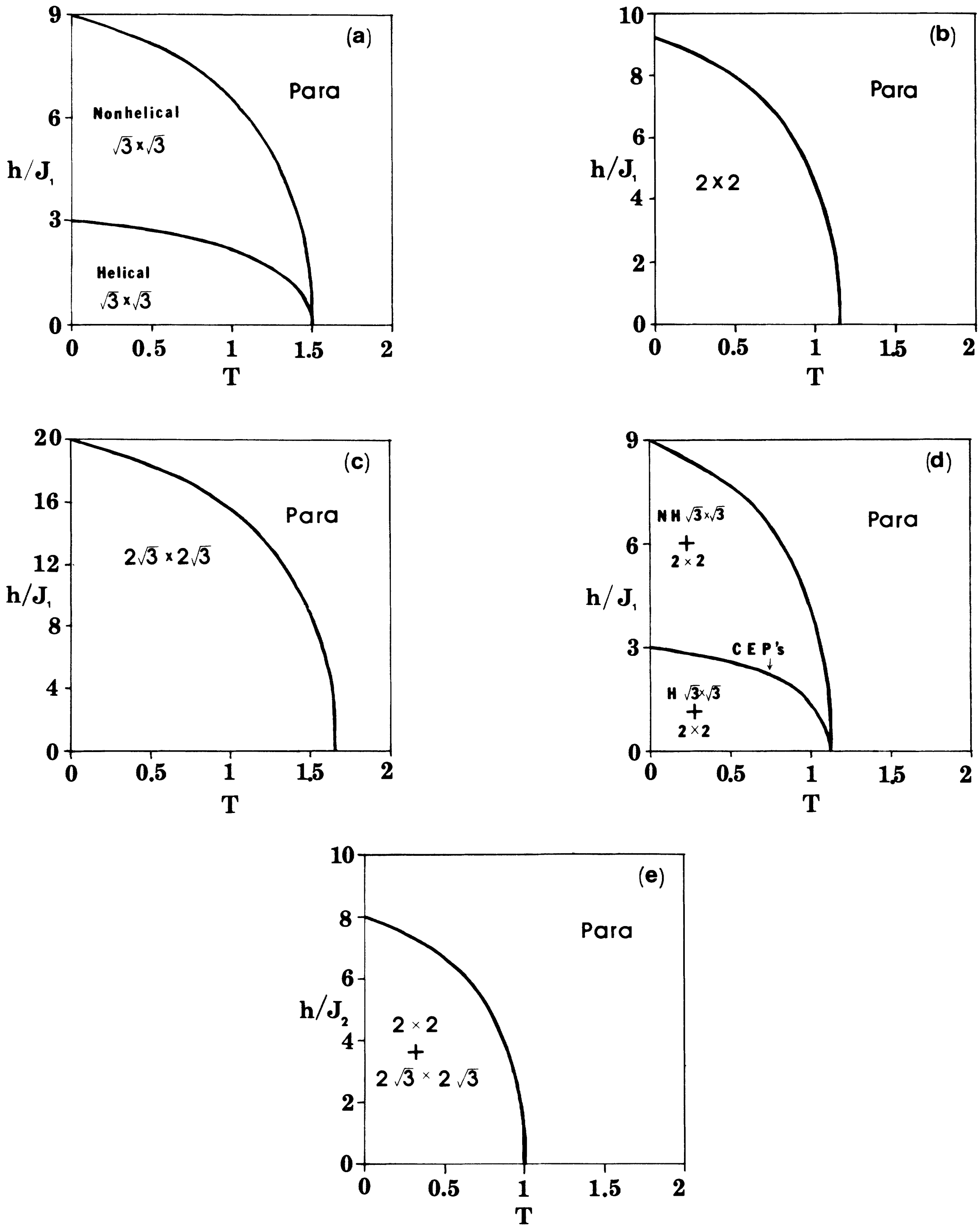

FIG. 4. The h vs T phase diagrams of five types are displayed. Units are chosen to be dimensionless. (a) $J_1=1/T$, $J_2=0$, $J_3=0$; (b) $J_1=1/T$, $J_2=0.15/T$, $J_3=0$; (c) $J_1=1/T$, $J_2=1/T$, $J_3=(\frac{7}{9})/T$; (d) $J_1=1/T$, $J_2=(\frac{1}{8})/T$, $J_3=0$; (e) $J_1=0$, $J_2=1/T$, $J_3=0$. Para stands for the paramagnetic phase. CEP stands for critical end point.

solution was best at $h=0$. Notice also that this phase has the helicity inherited from the $\sqrt{3}\times\sqrt{3}$ aspect.

For general h it is possible to construct the solution

$$X \equiv M/R(a) \ , \tag{12a}$$

$$1+\tau^2 \equiv 4/(3X^2+1) \ , \tag{12b}$$

$$\phi_0 \equiv \cos^{-1}X \ , \tag{12c}$$

$$e^{i\phi_\pm} \equiv (3X - e^{i\phi_0})\tfrac{1}{2}(1\pm i\tau) \ , \tag{12d}$$

$$\phi_1 = -\phi_2 = \phi_3 = -\phi_4 = \phi_0 \ , \tag{12e}$$

$$\phi_8 = -\phi_7 = \phi_{12} = -\phi_{11} = \phi_+ \ , \tag{12f}$$

$$\phi_{10} = -\phi_9 = \phi_6 = -\phi_5 = \phi_- \ . \tag{12g}$$

After applying lattice symmetries there are a large number of such equivalent states. These sublattices all have zero helicity (for $X > \frac{1}{3}$) or all have nonzero helicity (for $X < \frac{1}{3}$). There are some pairings of spins here, but not in a way to change the periodicity from $2\sqrt{3}\times 2\sqrt{3}$. It is unclear whether a continuum of solutions exists. It is possible that the a_k's are not independent of k for some solutions, but this case is too difficult to solve. If such (nonuniform) continua existed for $h\neq 0$, and they kept the helicity, then there would be two degenerate phases, just as in the simple nearest-neighbor problem.[1]

3. *Ferrimagnetic solutions*

The 2×2 and $\sqrt{3}\times\sqrt{3}$ solutions can be completely accounted for (see Fig. 3). Besides the uniform continua all the other states (denoted as ferrimagnetic in Table I) have the spins parallel or antiparallel to the magnetic field direction. Any structure in the ferrimagnetic states must involve the magnitude of the a_k's. Furthermore, these states do not have the infinite degeneracy of the continuum states. These ferrimagnetic states can be found by computer and the continuum states can be found analytically. Also, in the $\sqrt{3}\times\sqrt{3}$ ordering there is also a helical transition similar to that discussed in Ref. 1.

4. *Possibility of other solutions*

I have given a complete classification of the available solutions with 1×1, 2×2, or $\sqrt{3}\times\sqrt{3}$ symmetry. I have also accounted for all phases with uniform a_k. This leaves only phases with either $2\sqrt{3}\times\sqrt{3}$ or $2\sqrt{3}\times 2\sqrt{3}$ symmetry that do not have uniform a_k. At this point, I cannot say much about such phases, if they exist.

III. RESULTS

With the above classification of the possible solutions, it is now appropriate to examine the possible phase diagrams. Portions of the J_1,J_2,J_3,h phase space have been examined with the aid of a computer. The computer scans wide portions of an h versus T cross section for given ratios of J_1, J_2, J_3. At each point all the phases which can be found are compared, in order to find the lowest value of the free energy Ψ. As long as the correct global minimum is examined, it is irrelevant how many "bad guesses" are checked.

In all cases examined, the ferrimagnetic solutions were never the global minima. It is possible that they are always saddle points of Ψ, but this has not been proven. This is the most difficult portion of the numerical calculations, however.

On the other hand, the 2×2, $\sqrt{3}\times\sqrt{3}$, and $2\sqrt{3}\times 2\sqrt{3}$ have been described well enough to easily and unequivocally find them. Examples of each of these are shown in Fig. 4. There are also rather interesting phase diagrams shown, in which there are entire regions of coexistence. Although not shown here, the same type of diagram also exists for the $\sqrt{3}\times\sqrt{3}$ and $2\sqrt{3}\times 2\sqrt{3}$ coexistence. These special coexistences result because of the special orientation of the coexistence "surface" in the full J_1,J_2,J_3,h space. It occurs only for very special choices of J_1,J_2,J_3,h, and is not a violation of the Gibbs phase rule. When this coexistence region contains a helical transition, then this helical transition line is actually a line of critical end points (CEP's) in the full space. There are even very special conditions under which all three of these ordered phases can coexist in the same region. This very rich behavior means that when corrections to mean field are applied, different cross sections will probably cut through in different ways, and a multitude of rich behavior must be present.

These calculations suggest the range of interactions suitable to observe a $2\sqrt{3}\times 2\sqrt{3}$ phase in the $MnCl_2$ experiments may be

$$\begin{aligned} -J_1+2J_2+3J_3 &> 2J_1+2J_2-6J_3 \ , \\ -J_1+2J_2+3J_3 &> 3J_1-6J_2+3J_3 \ . \end{aligned} \tag{13}$$

A more precise statement could be made by attempting to fit the curves to the experimental data. This has not been done.

There are at least two modifications that can be done to improve the results while staying in the above formalism. First, vacancies may be allowed for, so that spins are absent from some sites. Secondly, interactions of spins in different layers may be taken into account. Of course if there is any reason to expect other periodicities or incommensuration, then that must be handled. But that was not observed experimentally for the case I am considering. Such modifications are left for the future.

One can argue that the mean-field theory cannot obtain the Kosterlitz-Thouless (KT) behavior correctly, and thus it should be abandoned. But the structural ordering observed is believed to be in addition to the KT behavior and thus is probably not invalidated. Monte Carlo estimates of the nearest-neighbor problem bear this out, and give good agreement with most of the mean-field predictions.

ACKNOWLEDGMENTS

This work was done at the University of Rhode Island under support of National Science Foundation (NSF) Grant No. DMR8704730. This research was conducted using the Cornell National Supercomputing Facility, a resource of the Center for Theory and Simulation in Science and Engineering at Cornell University, which is funded in part by the NSF, New York State, and the IBM Corporation.

---

*Current mailing address: Exxon Production Research, P.O. Box 2189, Houston, TX 77252-2189.

[1]D.-H. Lee, R. G. Caflisch, J. D. Joannopoulos, and F. Y. Wu, Phys. Rev. B **29**, 2680 (1984).

[2]R. G. Caflisch, Phys. Rev. B **34**, 3185 (1986).

[3]Y. Kimishima, A. Furukawa, H. Nagano, P. Chow, D. Wiesler, H. Zabel, and M. Suzuki, Proceedings of the International Symposium of Graphite Intercalation Compounds, Tsukuba, Japan, 1985 [Synth. Metals **12**, 455 (1985)].

[4]S. Katsura, T. Ide, and T. Morita, J. Stat. Phys. **42**, 381 (1986).